Journal of Advanced Research 22 (2020) 47–55

Contents lists available at ScienceDirect

Journal of Advanced Research

journal homepage: www.elsevier.com/locate/jare

Pulsed high-power microwaves do not impair the functions of skin normal and cancer cells *in vitro*: A short-term biological evaluation

Sohail Mumtaz [a], Pradeep Bhartiya [b], Neha Kaushik [c], Manish Adhikari [b], Pradeep Lamichhane [a], Su-Jae Lee [c], Nagendra Kumar Kaushik [a,b,*], Eun Ha Choi [a,b,*]

[a] Department of Electrical and Biological Physics, Kwangwoon University, Seoul 01897, Republic of Korea
[b] Plasma Bioscience Research Center, Applied Plasma Medicine Center, Department of Plasma Bio Display, Kwangwoon University, Seoul 01897, Republic of Korea
[c] Department of Life Science, Hanyang University, Seoul 04763, Republic of Korea

HIGHLIGHTS

- Pulsed high power microwave (MW) at a frequency 3.5 GHz was generated.
- MW did not induce cell death in skin fibroblast normal cells and melanoma cells.
- MW did not alter the morphology of melanoma cells.
- Gene expression related to ATP synthesis and proliferation can get altered by MW.
- MW selectively stimulated viability and proliferation of only melanoma cells.

GRAPHICAL ABSTRACT

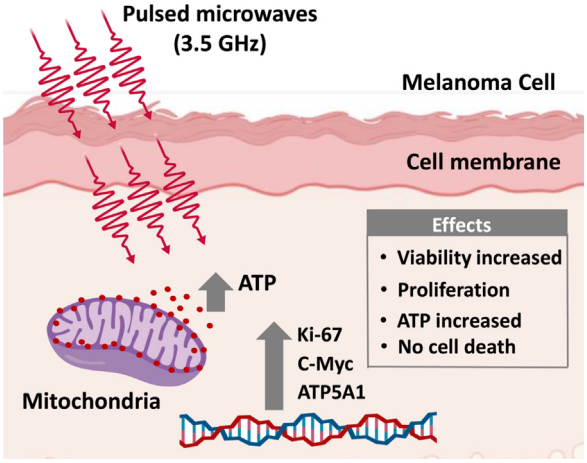

ARTICLE INFO

Article history:
Received 1 September 2019
Revised 14 November 2019
Accepted 17 November 2019
Available online 20 November 2019

Keywords:
Electromagnetic energy
Melanoma cell
Fibroblast skin cell
Proliferation
Adenosine triphosphate
Mitochondrial activity

ABSTRACT

Over the past few decades, microwave (MW) radiation has been widely used, and its biological effects have been extensively investigated. However, the effect of MW radiation on human skin biology is not well understood. We study the effects of pulsed high-power microwaves (HPMs) on melanoma (G361 and SK-Mel-31) and normal human dermal fibroblast (NHDF) cells. A pulsed power generator (Chundoong) was used to generate pulsed HPMs (dominant frequency: 3.5 GHz). For treatment 1, 5, 15, and 45 shots are given to cells in which the electromagnetic energy of 0.6 J was delivered to the cells at each trigger shot. Cell viability, proliferation rate, apoptosis, cell death, metabolic activity, and oxygen-free radical regulation were evaluated after the MW exposure at low and high doses. MW exposure increased the viabilities and proliferation rates of both melanoma cell lines in a dose-dependent manner, while no significant effects on the fibroblast cells were observed. We found an elevated level of ATP and mitochondrial activity in melanoma cells. Also, it was observed that MW exposure did not affect cell death in melanoma and fibroblast cells. A polymerase chain reaction analysis indicated that the MWs induced dose-dependent proliferation markers without affecting the cell cycle and apoptotic genes in

Peer review under responsibility of Cairo University.
* Corresponding authors.
E-mail addresses: kaushik.nagendra@kw.ac.kr (N.K. Kaushik), ehchoi@kw.ac.kr (E.H. Choi).

https://doi.org/10.1016/j.jare.2019.11.007
2090-1232/

the melanoma cells. Our findings show the differential effects of the MW radiation on the melanoma cells, compared to those on the fibroblast cells.

Introduction

Microwave (MW) radiation, referred to as nonionizing electromagnetic radiation, in the frequency range of 300 MHz–300 GHz has been extensively used in daily life for different purposes including domestic (food), industrial (telecommunications, agriculture, military), and medical purposes [1,2]. The popularization of cell phones, wireless devices, computers, and other electrical equipment has made the learning, working, and entertainment more convenient, but led to frequent exposure to MWs. Moreover, with the development of various advanced military weapons, equipment, and radars, the soldiers are exposed to intricate environmental factors, including high-power microwave (HPM) radiations [1]. MW radiation, which induces many biological effects, was considered the fourth largest source of pollution [3,4].

MWs can be used for medical purposes [2,5–7]. MW sensing and imaging have been used for tumor detection, early diagnostics, blood clot/stroke detection, heart imaging, bone imaging, and localization of in-body radio-frequency sources [8–17]. MW-based hyperthermia and its combination with chemoradiotherapy have been used as noninvasive cancer treatments to induce cancer cell apoptosis or cause the direct destruction of tumor cells or reduction in nodule volume for the treatment of benign thyroid nodules [18–24]. MWs have been also used in the early detection and imaging of breast cancer by dual-mode or thermoacoustic imaging model. Continuous MW exposure could be beneficial for biological functions such as an increase in the healing of wounds (septic and aseptic) and intracranial hematoma detection [8–17].

MWs also have considerable health-damaging effects, particularly on the nervous system [21–30]. Long-term MW exposure or MW radiation in the range of 860–2450 MHz had significant effects on the brain, such as inductions of hippocampus injury, neurotransmitter disruption, and cognitive impairment [21–30]. Pulsed and dose-dependent MWs affect the autoimmunity and immunomodulation by functional and morphological injuries in the natural killer (NK-92) [31]. Kerimoglu et al. reported that continuous exposure to an electromagnetic field impairs the morphological and biochemical levels [32]. Wang et al. investigated the effect of pulsed MWs on bone marrow cells at a frequency of 2.856 GHz [33]. Szymanski *et al.* reported the electromagnetic immunomodulatory effects on atopic-dermatitis-modified keratinocytes [34]. In addition, MW radiation can induce skin cancer in mice and brain tissues [35]. Various mathematical models also studied which helps to realize the dynamical procedures of biology population changes [36–41]. Skin is located on the outermost layer of the body, which exposed frequently to the physical stimuli, toxic chemicals, radiations with short and long wavelengths, and environmental contaminations. The effects of sunlight on the skin have been well established [42–45]. Radiations with longer wavelengths are gathering attention for their effects on skin health. However, the effect of the pulsed HPM radiation with nanosecond pulse duration is largely unknown in skin biology.

In this study, we aimed to determine the effects of pulsed HPM with nanosecond pulse duration at a frequency of 3.5 GHz on melanoma and fibroblast cells. The possible effects at cellular and molecular levels were evaluated with respect to the cellular growth and energetics. We assessed the cell viability, apoptosis, proliferation and cell death, and adenosine triphosphate (ATP) level.

Materials and methods

Cell culture

Human melanoma cell lines G-361 (ATCC® CRL-1424™) and SK-Mel-31 (ATCC® HTB-73™) were purchased from Korean Cell Line Bank. A normal human dermal fibroblast (NHDF) cell line (Cat # CC-2511) was purchased from Lonza (Walkersville, Maryland, USA). All cell lines were cultured and stored according to the manufacturers' protocols. The G-361, SK-Mel-31, and NHDF cells were cultured in Roswell Park Memorial Institute 1640 with 10% fetal bovine serum (FBS), 100 U/mL of penicillin, and 100 μg/mL of streptomycin, minimum essential medium supplemented with 15% FBS, 100 U/mL of penicillin, and 100 μg/mL of streptomycin, and fibroblast basal medium with supplied 100 U/mL of penicillin and 100 μg/mL of streptomycin, respectively. Cells were maintained in a humidified incubator at 37 °C with 5% CO_2 and subcultured every three to four days.

MW exposure system

Various sources can be used to generate HPMs. Among them, the virtual cathode oscillator (vircator) was considered as the most promising source owing to its ability to generate MWs with high power. In this study, an axial vircator was designed for the generation of MWs. A relativistic HPM generator device (Chundoong) was used. This device uses a relativistic electron beam to generate MWs having high power in the range of several hundred megawatts to gigawatt levels [46–48]. Fig. 1 shows a schematic of the device used in this study. Marx bank consisted of 12 capacitors; each capacitor had a capacitance of 0.2 μF. It utilized a high voltage when the capacitors were discharged in the series with a trigger shot after 1 min of charging at a voltage of 20 kV. In this device, the characteristics of relativistic electron beam reached the maximum values (voltage of 600 kV, current of 88 kA, and pulse duration of 60 ns) when the characteristic impedance (6.8 Ω) of the pulse-forming line (PFL) was matched to that of the field-emission diode in vacuum [46,47]. The drift tube had a length of 25 cm and an inner diameter of 20 cm. Diode and drift tube regions were evacuated down to 1.5×10^{-5} Torr in this experiment. The end part of the drift tube was sealed using an acrylic window with a thickness of 1.5 cm to maintain the vacuum and electron bombardment. It also allowed MW to propagation outside the drift tube. Targat sample was placed 25 cm away from the window where it was exposed to different doses of electromagnetic energy by varying the number of shots 1, 5, 15, and 45 shots (each shot given after one minute) of pulsed MW radiation (1 shot = 0.6 J). The temperature of the cell medium is measured by using a thermal imager FLUKE Ti90. The temperature was measured by placing the cell medium in the treatment room when the room temperature is 25 °C. After 5-min and 45-min placing the cell medium, the temperature of the cell medium was measured in two conditions, without MW exposure (control) and with microwave exposure (treated).

Cell viability assay

Alamar blue (AB; ThermoFisher Scientific DAL1025) dye was used to assess the viabilities of the melanoma and fibroblast cells

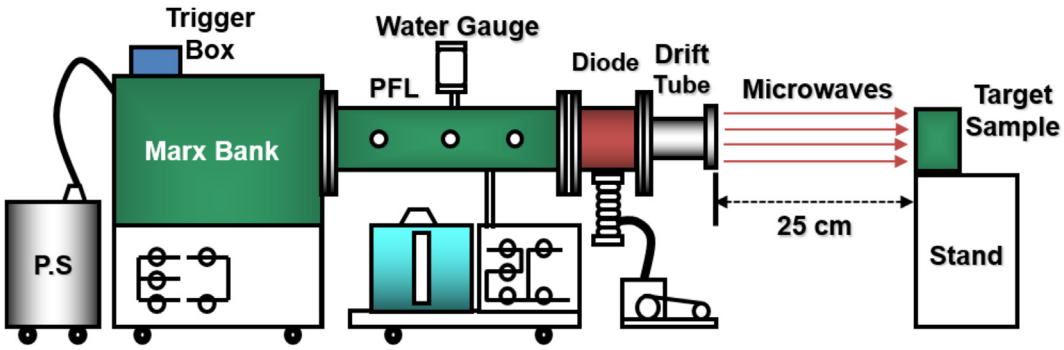

Fig. 1. Schematic of the MW exposure device (Chundoong).

upon the exposure to MWs. For the AB cell viability experiments, all cells (G-361, SK-Mel, and NHDF) were seeded at a density of 5×10^3 cells per well (100 μL) in 96-well plates. We performed the experiments in triplicates (or more); each set contained a control (unexposed to MWs). After 5, 24, 48, and 72 h of incubation, the medium was removed, and the cells were washed with a prewarmed 1X Dulbecco phosphate-buffered saline (PBS, Welgene Cat # LB 001-02) with pH 7.4. An AB solution (10% v/v) was prepared in the medium, added to each well according to the manufacturer's instructions and incubated for 1 h as carried out in our previous work [49]. The AB conversion was measured by a plate-reading spectrometer (BioTek) by monitoring the fluorescence as a measure of the AB dye conversion using 540-nm excitation and 595-nm emission.

Cell death and apoptosis assay

Cell death upon the MW exposure was determined by evaluating the propidium iodide (PI) uptake of the cells. PI was commercially purchased (Sigma Aldrich, Germany) and prepared in PBS (Gibco) at a concentration of 1 mg/mL as a working stock solution. For fluorescence-activated cell sorting, 2×10^4 cells/well of G361, SK-Mel-31, and NHDF (12 wells for each sample) were seeded in 96-well plates. After 24 h of MW exposure, the cells were washed with PBS and harvested using 0.25% trypsin–ethylenediaminete traacetic acid (HyClone, Cat # SH30042.01) for 2–3 min, followed by the addition of the medium supplemented with 10% FBS to neutralize the effects of trypsinization and centrifugation to obtain a pellet. The pellet was resuspended with PBS containing PI and subjected to flow cytometry acquisition and analysis. In addition, the apoptosis of the cells was determined using a Real-Time-Glo™ Apoptosis kit (Promega (Ref JA1011)). This assay enables the luminescence-based detection of phosphatidyl-serine exposure indicative of apoptosis of the cells. For this purpose, 5×10^3 cells/well of G361 were seeded in 96-well plates in octuplicates. After 24 h of MW exposure, an equal amount of 2X detection reagent was added to media, mixed, and incubated in a humidified incubator at 37 °C with 5% CO_2. The luminescence was measured using a BioTek microplate reader.

ATP assay

ATP generation was assessed following the manufacturer's protocol (Cell Titer-Glo® Luminescent Cell Viability Assay (Promega - G7572)). All (G-361 and SK-Mel) cells were seeded at a density of 5×10^3 cells per well (100 μL) in 96-well plates. After the exposure to MWs for 24 h of incubation, one volume of the prewarmed reagent was added to the cells. After 2 h of incubation at room temperature, the luminescence was measured using a microplate reader.

Proliferation assay

The cell growth was monitored using CellTiter 96 Aqueous One Solution – Promega (Ref G3580), a colorimetric method utilizing the interaction of 3-(4,5-dimethylthiazol-2-yl)-5-(3-carboxyme thoxyphenyl)-2-(4-sulfophenyl)-2H-tetrazolium with phenazine methosulfate to form a colored formazon product only in the presence of Nicotinamide adenine dinucleotide hydrogen/Nicotinamide adenine dinucleotide phosphate hydrogen from metabolically active cells. First, 5×10^3 cells/well of G361, SK-Mel-31, and NHDF were seeded in 96-well plates in octuplicates. Twenty-four hours after the seeding, the cells were exposed to MWs (5 and 45 shots) while the control cells were not exposed. After the MW exposure, the cells were incubated for 24 h at 37 °C in a humidified environment with 5% CO_2. At the end of the incubation, one-fifth of the volume of the CellTiter 96 Aqueous One solution was added into each well and incubated for 2 h. The absorbance at 490 nm (A_{490}) was measured using the Bio-Tek microplate reader.

Mitochondrial assay

Mammalian cells generate ATP by mitochondrial (oxidative phosphorylation) and nonmitochondrial (glycolysis) mechanisms. Mitochondrial ToxGlo™ Assay (Promega G8000) is a cell-based assay primarily used to predict mitochondrial dysfunction. The assay can be used to measure ATP generated by mitochondria, which can be indicative of mitochondrial activity. ATP is measured by adding the ATP detection reagent, leading to cell lysis and generation of a luminescent signal that is proportional to the amount of ATP. ATP detection reagent consists of an optimized formulation for ATP detection containing luciferin, ATPase inhibitors, and thermo-stable Ultra-Glo™ luciferase. For this assay, 5×10^3 cells/well of G361 were seeded in 96-well plates in octuplicates. After 24 h of seeding, the cells were exposed to MWs (5 and 45 shots), while the control cells were not exposed. After the MW exposure, the cells were incubated for 24 h at 37 °C in a humidified environment with 5% CO_2. At the end of the incubation, the cells were processed according to the manufacturer's protocol. The ATP levels were measured using a luminometer.

Superoxide dismutase (SOD) activity

The effect on the production of free oxygen radicals was assessed by measuring the SOD activity using an Enzychrome (ESOD-100) assay kit (colorimetric assay). In the assay, superoxide (O_2^-) is provided by xanthine oxidase, which reacts with the water-soluble tetrazolium (WST)-1 dye to form a colored product. First, 5×10^3 cells/well of G361 were seeded in 96-well plates in triplicate. Twenty-four hours after the MW exposure, the cells were washed

with a cold PBS, lysed with a cold lysis buffer, and then centrifuged to obtain the supernatant of cellular extract. Subsequently, 20 μL of the supernatant was mixed with the working reagent (including the assay buffer, xanthine, and WST-1). Xanthine oxidase was added to each sample and mixed. The absorbance at 440 nm (A_{440}) was measured after 0 and 60 min, according to the manufacturer's protocol.

Molecular analysis (reverse-transcription polymerase chain reaction (PCR))

Ribonucleic acid (RNA) was isolated from the samples using the Trizol reagent (Ambion). An RNA quantification was performed using a NanoDrop™ spectrophotometer according to the manufacturer's protocol. All real-time PCRs were determined using an SYBR Green Master Mix (Biorad Laboratories, Inc., Korea). Sample amplification reactions were carried out in a Rotor Gene Q (Qiagen, Korea). The results are expressed as the fold change calculated by the ΔΔCt method relative to the control sample. β-actin was used for normalization as a control. The primer sequences are listed in Table 1.

Statistical analysis

The experimental results were plotted using the Microsoft Excel software (2013, for Windows) and Graph Pad Prism as the mean ± standard error of three independent experiments. The significance was assessed using the Student's *t*-test. The differences were considered statistically significant when p was lower than 0.05 (p values: $^{*}P < 0.05$, $^{**}P < 0.01$, $^{***}P < 0.001$).

Results

Physical characteristics of the MW exposure device

Fig. 2(a) shows the peaks of the diode voltage (260 kV) and diode current (10 kA). The target sample was placed 25 cm away from the acrylic window. At each trigger shot, an HPM pulse was generated, which propagated toward the target sample. The average power of the MWs reaching the target sample at each trigger shot was 20 MW, as shown by the microwave envelope signal in Fig. 2(b), which corresponds to an electromagnetic energy delivered to the cells at each trigger shot of approximately 0.6 J. The MW generation from vircator was described in details in our previous studies [46,48]. The dominant frequency of the MWs was 3.5 GHz, determined by fast Fourier transform. The frequency spectrum is shown in Fig. 2(c). The measured temperatures of the cell medium before and after the MW exposure are shown in Fig. 2 (d) (the room temperature was 25 °C). After 5-min and 45-min temperature was measured in the cell medium without MW exposure in control and with microwave exposure in the treatment group. The temperature of the cell medium does not show any change after the exposure because of the nanosecond pulse duration of MW and 1 min gap between each shot.

Table 1
List of used primers. β-actin was kept as an endogenous control for the qPCR experiment (L = forward primer; R = reverse primer).

Gene	Sequence
Ki67_L	5′- CCT TCA GCC ACG ATT TCA GG -3′
Ki67_R	5′- TTG GGG AAC ACA GAG AGG AC -3′
Cmyc_L	5′- CAC ATC AGC ACA ACT ACG CA -3′
Cmyc_R	5′- TTG TGT GTT CGC CTC TTG AC -3′
Casp3_L	5′- ATG TCG ATG CAG CAA ACC TC -3′
Casp3_R	5′- TCC TTC TTC ACC ATG GCT CA -3′
Casp9_L	5′- CGA CAT CTT TGA GCA GTG GG -3′
Casp9_R	5′- GAA AGC TTT GGG GTG CAA GA -3′
ATP5A1_L	5′- TTT TGC CCA GTT CGG TTC TG -3′
ATP5A1_R	5′- GAT ATC CCC TTA CAC CCG CA -3′
CDC2_L	5′- CTT TAG CGC GGT GAG TTT GA -3′
CDC2_R	5′- GTT CCT CAT ACT CGC CCT CC -3′
CENPF_L	5′- CTC ACC CAG GAG TTA CAG CA -3′
CENPF_R	5′- TCT CCT TGA TCT GAC TCG CC -3′
ATP2B1_L	5′- AGG TCT GTT GAT GTC TGC CA -3′
ATP2B1_R	5′- GCA CTG CGA CCA CTA AAA CT -3′

Effects of the HPM radiation on the viabilities of the melanoma and fibroblast cells

In this work, the melanoma (G-361 and SK-Mel-31) and fibroblast (NHDF) cells were exposed to the pulsed HPMs at low and high doses of electromagnetic energy. The cell viability was determined by the AB assay. The dose-dependent behaviors of the melanoma G361 and NHDF cells were evaluated 24 h after the MW exposure, as shown in supplementary Fig. S1. Based on these results, the low dose of 5 shots and a high dose of 45 shots were used in further investigations. The obtained results 5 h after the MW exposure (Fig. 3(a), (e), and (i)) show that the viability of the MW-exposed melanoma cells was increased compared to that of the control cells. The low dose of MW exposure did not significantly affect the NHDF cells, while the high dose changed the viability of the NHDF cells to a significant level. Fig. 3(b), (f), and (j) show the viabilities of the cells 24 h after the MW exposure. The cell viability continued to increase. High dose of MW exposure led to a significantly higher viability than that of the unexposed melanoma G-361 cells, without affecting the morphology (Fig. S2). The SK-Mel-31 cells exhibited an increased viability at the high dose, while the effect of the low dose was insignificant. On the other hand, the NHDF cells did not exhibit significant changes in viability at both low and high doses after 24 h. Further, incubation after the MW exposure was prolonged and cell viabilities were determined after 48 and 72 h (Fig. 3(c), (g), and (k) and (d), (h), and (l), respectively). Notably, no significant changes in the MW-exposed groups were observed, compared to the unexposed groups of both melanoma (G-361 and SK-Mel-31) and fibroblast cells. The figures show that the MW exposure at the high dose led to slightly increased viabilities of the melanoma (G-361 and SK-Mel-31) and fibroblast (NHDF) cells after 5 h. The maximum value was observed after 24 h for the G-361 cells at a high dose. The melanoma G361 and SK-Mel-31 cells exhibited similar responses indicated by the viability patterns at the early time moment, 5 h after the exposure. A significant proliferation of the G361 cells was observed after 24 h, while no significant changes were observed after 48 and 72 h. The NHDF cells reacted to the MW exposure at the early time moment, while no significant changes were observed after the prolonged incubation. Considering these results, the G-361 cells exposed to the MW radiation (5 and 45 shots) and incubated for 24 h were used in the subsequent experiments.

Effect of the HPM radiation on the cell death

To investigate whether the MW exposure leads to death of the melanoma and fibroblast cells, the cells were seeded in 96-well plates, exposed to MW radiations (5 and 45 shots), and incubated for 24 h. The cell death induced by the MW exposure until 24 h of incubation after the exposure was determined by the PI uptake, indicative of a dysfunctional plasma membrane. As shown in Fig. 4(a) and (b), the histogram analysis indicates no significant variations in the MW-exposed groups with respect to the control groups of both melanoma cell populations. In addition, the scatter plot for the fibroblast cells shows insignificant variations in the MW-exposed groups compared to the control (Fig. 4(c)). Overall,

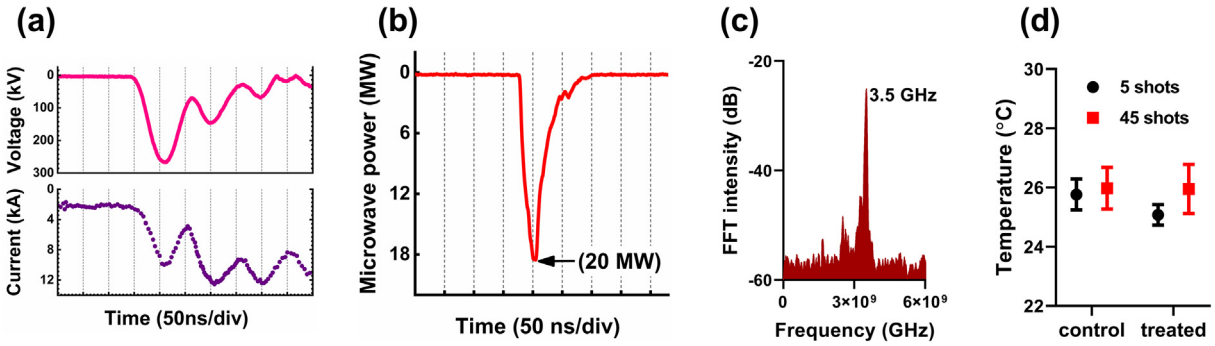

Fig. 2. Physical characteristics of the MW exposure device. (a) Traces of the diode voltage and diode current, (b) MW envelope signal, (c) frequency spectrum of the MWs, and (d) temperatures of the cell medium before and after the MW exposure (the room temperature was 25 °C).

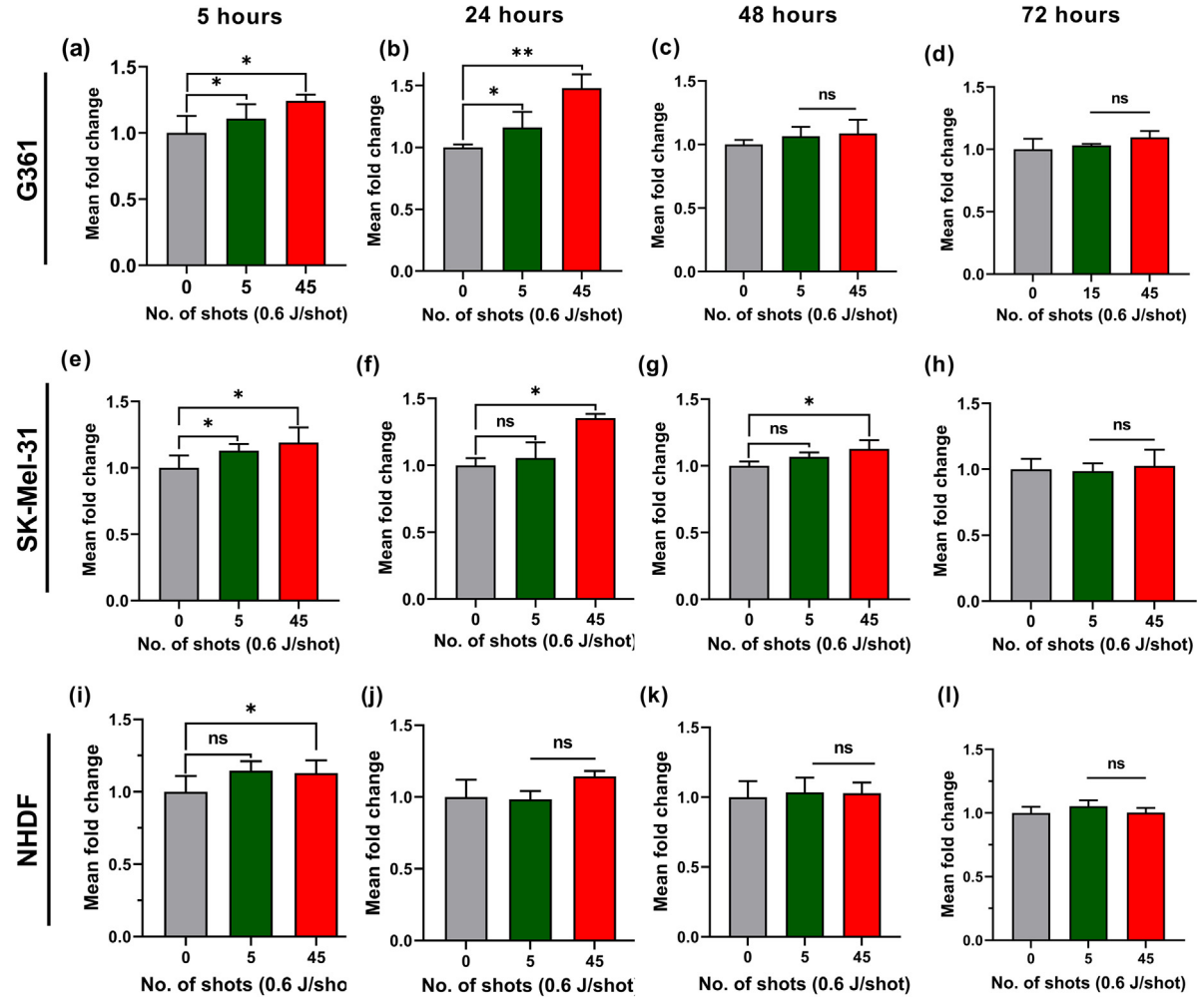

Fig. 3. Effects of the pulsed HPMs on the viabilities of the melanoma and fibroblast cells. The melanoma (G-361 and SK-Mel-31) and fibroblast (NHDF) cells were exposed to the pulsed MWs (5 and 45 shots; 0.6 J/shot). The cell viabilities were evaluated 5, 24, 48, and 72 h after the 5 and 45 shots of MW exposure; the results are compared with those for the control. (a–d), (e–h), (i–l) Viabilities of the melanoma G-361 and SK-Mel-31 and NHDF cells in the range of 5–72 h, respectively (n = 3). The significance was calculated using Microsoft Excel (MS Office 2010). The differences between the treatment groups are indicated by $^{*}P < 0.05$, $^{**}P < 0.01$, $^{***}P < 0.001$.

the death of melanoma and fibroblast cells was not observed after the pulsed MW exposures at both low and high doses.

Effects of the HPM radiation on the mitochondrial energetics

To investigate whether the increase in proliferation of the melanoma cells after the MW exposure is attributed to changes in cellular energetics, the proliferation, apoptosis, mitochondrial activity, ATP level, and oxygen radical regulation were assessed using the CellTiter 96 Aqueous One Solution, Promega Apoptosis, Mitotox and ATP, CellTiter-Glo® Luminescent Cell Viability, and Enzychrome SOD activity assays, respectively. As shown in Fig. 5 (a), the ATP levels, indicative of proliferation, were high in the MW-exposed groups, which did not exhibit alteration in apoptotic

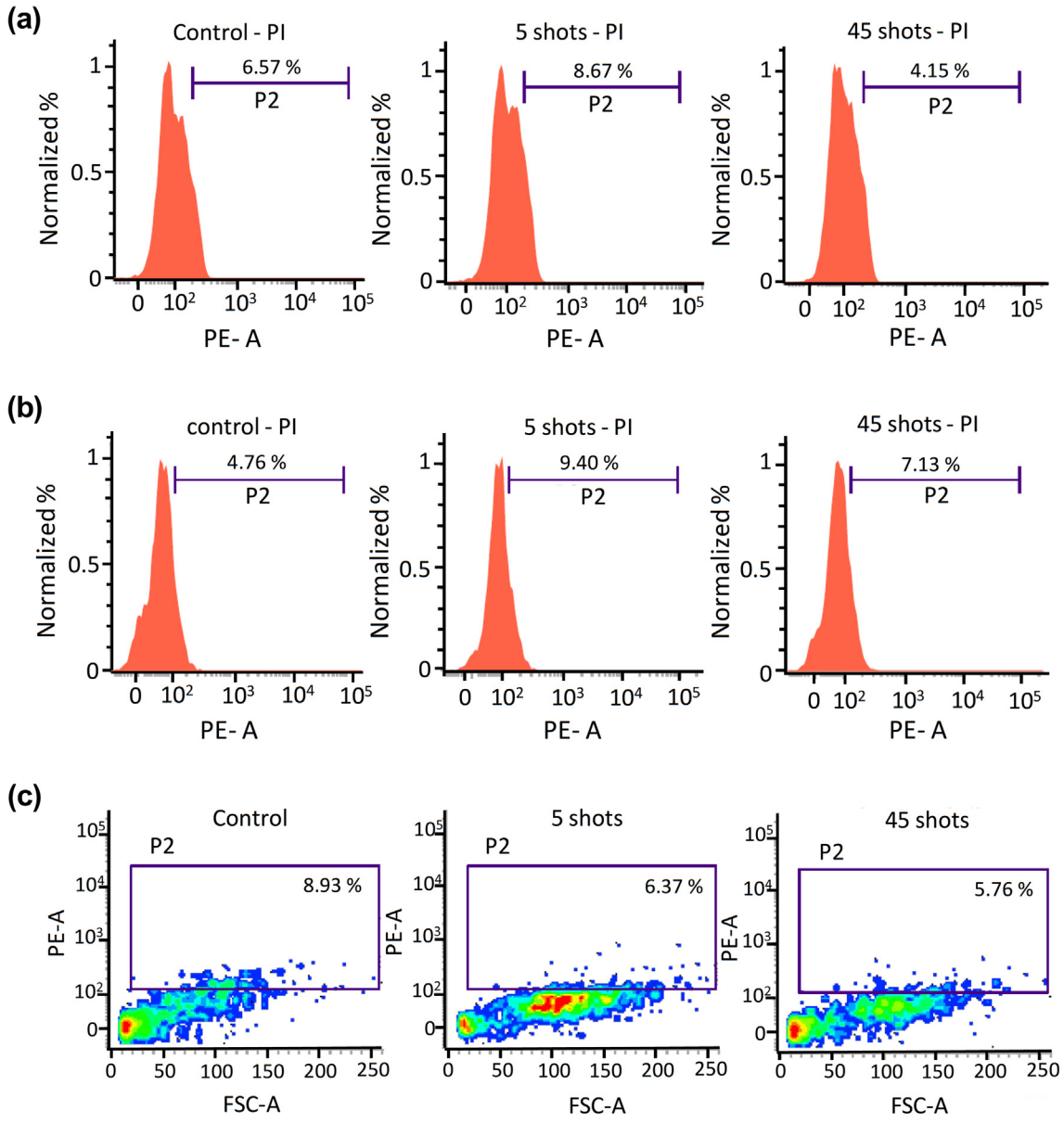

Fig. 4. Effects of the MW exposure on the death of melanoma and fibroblast cells. Representative histograms of the (a) G-361, (b) SK-Mel-31, and (c) NHDF cell populations after the MW exposure (n = 3). The significance was calculated using Microsoft Excel (MS Office 2010), while the differences between the treatment groups are indicated by $^{*}P < 0.05$, $^{**}P < 0.01$, $^{***}P < 0.001$.

rate (Fig. 5(b)). The mitochondrial released and cellular ATP levels are presented in Fig. 5(c) and (d), respectively. The ATP was also evaluated in SK-Mel-31 and NHDF 24 h after the MW exposure; the results are shown in Fig. S3.

ATP level was significantly increased only in the melanoma cells of the MW-exposed group, compared to that of the control group. We analyzed whether the increase in ATP level is associated with the antioxidant activity response of the cells. As shown in Fig. 5(e), the SOD activity level, indicative of primary antioxidant response, was unaffected upon the MW exposure. The figures indicate that the MW exposure enhanced the cellular proliferation possibly through the increased ATP level independent of the SOD activity in the melanoma cells, while the fibroblast cells were unaffected.

The above analyses demonstrate that the MW radiation remarkably affected the melanoma and fibroblast cells. In this regard, we aimed to analyze the mechanisms responsible for the differential effects on the cells. To this end, we performed a quantitative PCR (qPCR) analysis of the G361 melanoma cells and evaluated the MW effects on the proliferation, cell cycle regulation, and mitochondrial activity. Notably, the MW radiation considerably increased the Ki67 and cellular myelocytomatosis (c-Myc) proliferation gene levels, while the apoptotic genes caspase (CASP3) and (CASP9) and cell cycle regulatory genes were slightly affected or unchanged (Fig. 6(a) and (b)). The mitochondrial ATP synthase ATP5A1 level was significantly increased, while the Adenosine triphosphatase ATP2B1 level was significantly reduced upon the MW radiation, as shown in Fig. 6(c). Also, the cell division markers remain unaffected, as shown in Fig. 6(c). These data suggest that the increased levels of ATP are responsible for the enhanced ATP uptake in the melanoma cells in response to the MW radiation, as shown in Fig. 5(d).

Discussion

MW radiation increased the viability and proliferation of the melanoma cells within 24 h and its effect was reduced to insignif-

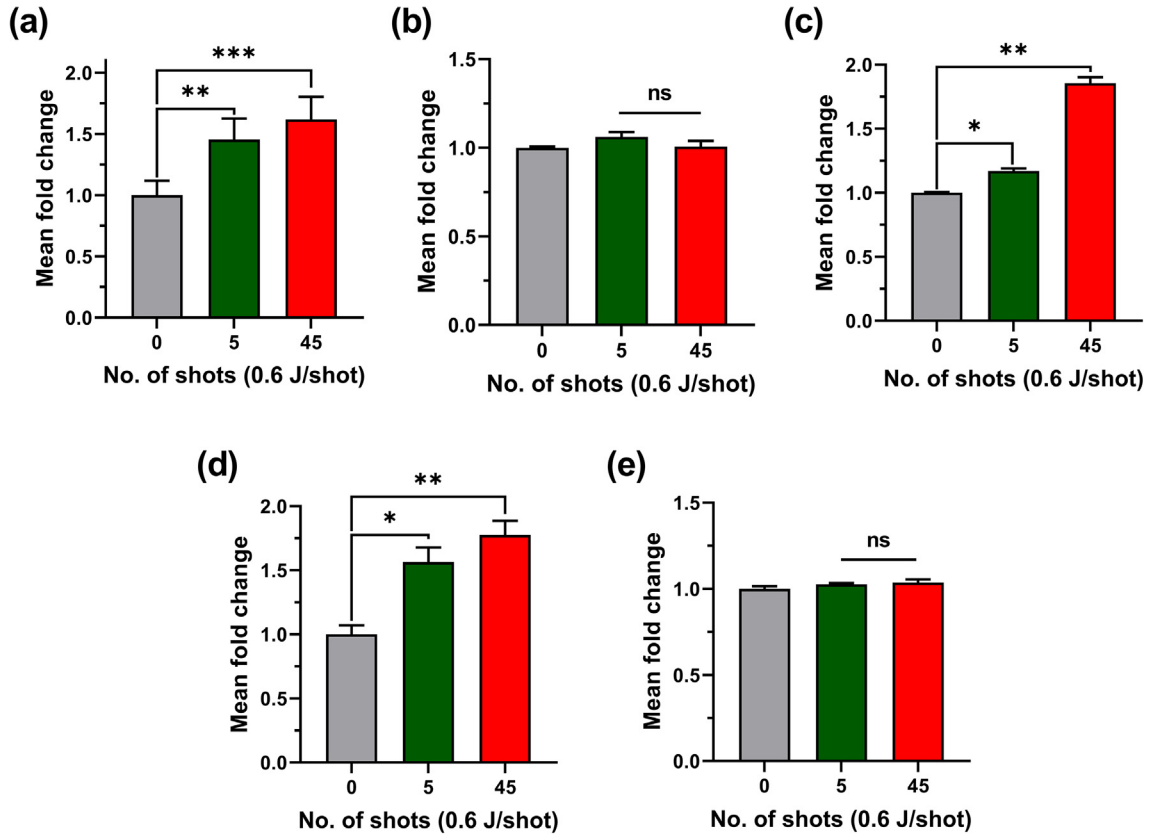

Fig. 5. Effects of the MW exposure on the mitochondrial energetics in the melanoma G-361 cells. The MW-exposed and control G-361 cells were evaluated after 24 h by different assays including the (a) proliferation, (b) apoptosis, (c) Mito, (d) relative ATP level, and (e) SOD level assays ($n = 3$). The significance was calculated using Microsoft Excel (MS Office 2010), while the differences between the treatment groups are indicated by $^{*}P < 0.05$, $^{**}P < 0.01$, $^{***}P < 0.001$.

icant levels after 48 and 72 h. The normal fibroblast cells were unaffected even after 72 h (Fig. 3). MWs could enhance the tumorigenesis of skin cancer [35]. In addition, low to moderate heat exposures induced heat shock protein expression, strongly associated with thermo-tolerance [50,51]. These results indicate highly proliferative and resistant structures of the melanoma cells towards heat. MW-induced hyperthermia-based treatments of melanoma could not achieve a significant disease-free survival rate or complete abolishment of cancer cells [18]. In our study, the viability and proliferation assay results showed the high proliferation ability of the melanoma cells after the MW exposure, while the proliferation rate of the normal fibroblast cells was unchanged. Yonezawa's group reported that the heating up to or above 43 °C could induce apoptosis only in malignant fibrous histiocytoma, compared to various soft tissue and osteosarcoma cell lines [52]. At least a few cell types could exhibit different sensitivities toward heat-induced cell death. Our study demonstrates that the MW exposure does not induce death of the melanoma and fibroblast cells (Fig. 4).

In this study, the ATP level and mitochondrial activity were increased 24 h after the MW exposure only in the melanoma cells, unlike in the fibroblast cells (Figs. 5 and S4). The mitochondrial activity and ATP level are directly correlated with cell growth and cell death [53]. A high ATP level leads to increased cell viability and proliferation, often used for its assessment [54–57]. Our results also showed high cellular and mitochondrial released ATP levels in response to the MW exposure of the melanoma cells in line with the increased viability and proliferation (Fig. 5). Notably, no significant changes in the ATP level in the normal fibroblast cells were observed. This indicates a larger sensitization of melanoma cells toward MWs than that of normalized fibroblast cells. Continuous exposure to an electromagnetic field or MWs can regulate cellular functions at the morphological, biochemical, and gene expression levels [54–57]. Our PCR results showed that the MW exposure of the melanoma cells enhanced the expressions of genes associated with proliferation and ATP synthesis without altering the genes required for cell cycle and apoptosis (Fig. 6). Also stimulus by any physical or chemical treatment may enhance ATP production and release in these cancerous cells. In this research proliferation of melanoma cancer cells is enhanced after exposure of pulsed MW, possibly this is the reason that ATP level is increased more in melanoma cells.

The cellular ATP level and mitochondrial function are often associated with SOD activity. The mitochondrial respiratory chain leads to the formation of reactive oxygen species, including hydroxyl radicals (OH·), superoxide ($O_{2}\cdot^{-}$), and peroxide (O_2^{2-}) [58]. SOD, a mitochondrially localized antioxidant enzyme, catalyzes the conversion of these superoxides to hydrogen peroxide and is upregulated owing to the mitochondrial dysfunction [59]. Melanoma cells tend to alter and adapt metabolic compensatory strategies for viability and growth [60]. Our results indicate that the MW exposure did not alter the SOD activity in the melanoma cells (Fig. 5). This result indicates alternative antioxidant mechanisms for the regulation of the levels of free radicals produced by mitochondria for an enhanced proliferation.

Conclusion

This study reveals that the MW exposure led to increased cell growth and proliferation specific to melanoma after 24 h, which could be attributed to the increased mitochondrial activity by the

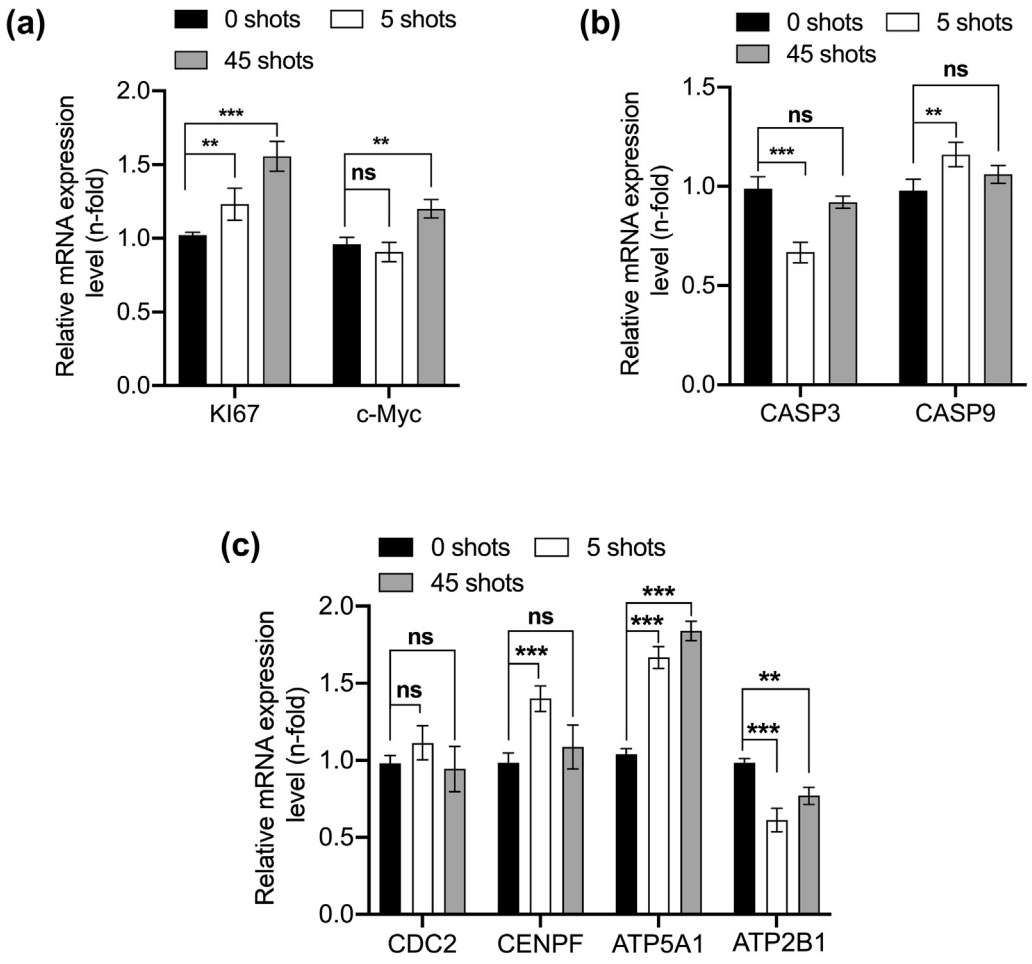

Fig. 6. Molecular analysis carried out to evaluate the effects of the pulsed HPM exposure on the cell proliferation, cell apoptosis, cell division and mitochondrial activity. (a) Proliferation markers Ki67 and c-Myc. (b) Apoptosis markers CASP3 and CASP9. (c) Cell division and mitochondrial markers cell division control (CDC) 2, centromere protein F (CENPF), ATP5A1, and ATP2B1. The significance was calculated between the treatment groups and indicated by $^{*}P < 0.05$, $^{**}P < 0.01$, $^{***}P < 0.001$.

increased ATP level. The MW exposure did not affect the normal fibroblast cells at the considered doses, while it altered the melanoma cell physiology in a cell-type specific manner. Therefore, MW exposure may be utilized with mitotic inhibitory chemotherapeutic drugs for melanoma cells and should be considered while analyzing melanoma cells *in vitro*. Further investigations are required to study the cellular signaling upon MW exposure.

Compliance with ethics requirements

This article does not contain any studies with human or animal subjects.

Acknowledgments

This study was supported by the National Research Foundation (NRF) of Korea, funded by the Korea government (MSIT) (NRF-2016K1A4A3914113, NRF-2019M3E5D1A01069361, NRF-2019R1I1A1A01043723), and by the Kwangwoon University, Seoul, Korea, through a Kwangwoon University Research Grant 2019–2020.

Declaration of Competing Interest

The authors have declared no conflict of interest

Appendix A. Supplementary material

Supplementary data to this article can be found online at https://doi.org/10.1016/j.jare.2019.11.007.

References

[1] Gubler H, Hiller M. The use of microwave FMCW radar in snow and avalanche research. Cold Reg Sci Technol 1984;9:109–19. https://doi.org/10.1016/0165-232X(84)90003-X.
[2] Osepchuk JM. A history of microwave heating applications. IEEE Trans Microw Theory Tech 1984;32:1200–24. https://doi.org/10.1109/TMTT.1984.1132831.
[3] United Nations Scientific Committee on the Effects of Atomic Radiation V (Austria). Ionizing radiation: sources and biological effects 1982 report to the General Assembly, with annexes. United States: United Nations; 1982.
[4] Balmori A. Electromagnetic pollution from phone masts. Effects on wildlife. Pathophysiology 2009;16:191–9. https://doi.org/10.1016/j.pathophys.2009.01.007.
[5] Tabuse K. Basic knowledge of a microwave tissue coagulator and its clinical applications. J Hepatobil Pancreat Surg 1998;5:165–72.
[6] Sterzer F. Microwave medical devices. IEEE Microw Mag 2002;3:65–70. https://doi.org/10.1109/6668.990689.
[7] Grenier K, Dubuc D, Chen T, Artis F, Chretiennot T, Poupot M, et al. Recent advances in microwave-based dielectric spectroscopy at the cellular level for cancer investigations. IEEE Trans Microw Theory Tech 2013;61:2023–30. https://doi.org/10.1109/TMTT.2013.2255885.
[8] Chandra R, Zhou H, Balasingham I, Narayanan RM. On the opportunities and challenges in microwave medical sensing and imaging. IEEE Trans Biomed Eng 2015;62:1667–82. https://doi.org/10.1109/TBME.2015.2432137.
[9] Bond EJ, Li X, Hagness SC, Van Veen BD. Microwave imaging via space-time beamforming for early detection of breast cancer. IEEE Trans Anten Propag 2003;51:1690–705. https://doi.org/10.1109/TAP.2003.815446.

[10] Fear EC, Li X, Hagness SC, Stuchly MA. Confocal microwave imaging for breast cancer detection: localization of tumors in three dimensions. IEEE Trans Biomed Eng 2002;49:812–22. https://doi.org/10.1109/TBME.2002.800759.

[11] Fhager A, Candefjord S, Elam M, Persson M. Microwave diagnostics ahead: saving time and the lives of trauma and stroke patients. IEEE Microw Mag 2018;19:78–90. https://doi.org/10.1109/MMM.2018.2801646.

[12] Semenov S, Kellam J, Althausen P, Williams T, Abubakar A, Bulyshev A, et al. Microwave tomography for functional imaging of extremity soft tissues: feasibility assessment. Phys Med Biol 2007;52:5705–19. https://doi.org/10.1088/0031-9155/52/18/015.

[13] Solberg LE, Aardal Ø, Berger T, Balasingham I, Fosse E, Hamran S. Experimental investigation into radar-based central blood pressure estimation. IET Radar, Sonar Navig 2015;9:145–53. https://doi.org/10.1049/iet-rsn.2014.0206.

[14] Semenov SY, Bulyshev AE, Posukh VG, Sizov YE, Willams TC, Souvorov AE. Microwave tomography for detection/imaging of myocardial infarction. I. Excised canine hearts. Ann Biomed Eng 2003;31:262–70.

[15] Obeid D, Sadek S, Zaharia G, El Zein G. Multitunable microwave system for touchless heartbeat detection and heart rate variability extraction. Microw Opt Technol Lett 2010;52:192–8. https://doi.org/10.1002/mop.24877.

[16] Zakrzewski M, Raittinen H, Vanhala J. Comparison of center estimation algorithms for heart and respiration monitoring with microwave doppler radar. IEEE Sens J 2012;12:627–34. https://doi.org/10.1109/JSEN.2011.2119299.

[17] Meaney PM, Zhou T, Goodwin D, Golnabi A, Attardo EA, Paulsen KD. Bone dielectric property variation as a function of mineralization at microwave frequencies. Int J Biomed Imag 2012;2012:649612. https://doi.org/10.1155/2012/649612.

[18] Hildebrandt B, Wust P, Ahlers O, Dieing A, Sreenivasa G, Kerner T, et al. The cellular and molecular basis of hyperthermia. Crit Rev Oncol Hematol 2002;43:33–56. https://doi.org/10.1016/S1040-8428(01)00179-2.

[19] Jha S, Sharma PK, Malviya R. Hyperthermia: role and risk factor for cancer treatment. Achiev Life Sci 2016;10:161–7. https://doi.org/10.1016/j.als.2016.11.004.

[20] Liu Y-J, Qian L-X, Liu D, Zhao J-F. Ultrasound-guided microwave ablation in the treatment of benign thyroid nodules in 435 patients. Exp Biol Med (Maywood) 2017;242:1515–23. https://doi.org/10.1177/1535370217727477.

[21] Hao Y-H, Zhao L, Peng R-Y. Effects of microwave radiation on brain energy metabolism and related mechanisms. Mil Med Res 2015;2:4. https://doi.org/10.1186/s40779-015-0033-6.

[22] Xiong L, Sun CF, Zhang J, Gao YB, Wang LF, Zuo HY, et al. Microwave exposure impairs synaptic plasticity in the rat hippocampus and PC12 cells through over-activation of the NMDA receptor signaling pathway. Biomed Environ Sci 2015;28:13–24. https://doi.org/10.3967/bes2015.002.

[23] Wang H, Peng R, Zhao L, Wang S, Gao Y, Wang L, et al. The relationship between NMDA receptors and microwave-induced learning and memory impairment: a long-term observation on Wistar rats. Int J Radiat Biol 2015;91:262–9. https://doi.org/10.3109/09553002.2014.988893.

[24] Guy AW, Chou C. Effects of high-intensity microwave pulse exposure of rat brain. Radio Sci 1982;17:169S–78S. https://doi.org/10.1029/RS017i05Sp0169S.

[25] Hinrikus H, Bachmann M, Tomson R, Lass J. Non-thermal effect of microwave radiation on human Brain. Environmentalist 2005;25:187–94.

[26] Deshmukh PS, Megha K, Nasare N, Banerjee BD, Ahmed RS, Abegaonkar MP, et al. Effect of low level subchronic microwave radiation on rat brain. Biomed Environ Sci 2016;29:858–67. https://doi.org/10.3967/bes2016.115.

[27] Odaci E, Hanci H, Ikinci A, Sonmez OF, Aslan A, Sahin A, et al. Maternal exposure to a continuous 900-MHz electromagnetic field provokes neuronal loss and pathological changes in cerebellum of 32-day-old female rat offspring. J Chem Neuroanat 2016;75:105–10. https://doi.org/10.1016/j.jchemneu.2015.09.002.

[28] Pall ML. Microwave frequency electromagnetic fields (EMFs) produce widespread neuropsychiatric effects including depression. J Chem Neuroanat 2016;75:43–51. https://doi.org/10.1016/j.jchemneu.2015.08.001.

[29] Terzi M, Ozberk B, Deniz OG, Kaplan S. The role of electromagnetic fields in neurological disorders. J Chem Neuroanat 2016;75:77–84. https://doi.org/10.1016/j.jchemneu.2016.04.003.

[30] Kivrak EG, Altunkaynak BZ, Alkan I, Yurt KK, Kocaman A, Onger ME. Effects of 900-MHz radiation on the hippocampus and cerebellum of adult rats and attenuation of such effects by folic acid and Boswellia sacra. J Microsc Ultrastruct 2017;5:216–24. https://doi.org/10.1016/j.jmau.2017.09.003.

[31] Zhao L, Li J, Hao YH, Gao YB, Wang SM, Zhang J, et al. Microwave-induced apoptosis and cytotoxicity of NK cells through ERK1/2 signaling. Biomed Environ Sci 2017;30:323–32. https://doi.org/10.3967/bes2017.043.

[32] Deniz OG, Kivrak EG, Kaplan AA, Altunkaynak BZ. Effects of folic acid on rat kidney exposed to 900 MHz electromagnetic radiation. J Microsc Ultrastruct 2017;5:198–205. https://doi.org/10.1016/j.jmau.2017.06.001.

[33] Wang C, Wang X, Zhou H, Dong G, Guan X, Wang L, et al. Effects of pulsed 2.856 GHz microwave exposure on BM-MSCs isolated from C57BL/6 mice. PLoS ONE 2015;10:e0117550. https://doi.org/10.1371/journal.pone.0117550.

[34] Szymanski L, Cios A, Lewicki S, Szymanski P, Stankiewicz W. Fas/FasL pathway and cytokines in keratinocytes in atopic dermatitis - manipulation by the electromagnetic field. PLoS ONE 2018;13:e0205103. https://doi.org/10.1371/journal.pone.0205103.

[35] Szmigielski S, Szudzinski A, Pietraszek A, Bielec M, Janiak M, Wrembel JK. Accelerated development of spontaneous and benzopyrene-induced skin cancer in mice exposed to 2450-MHz microwave radiation. Bioelectromagnetics 1982;3:179–91. https://doi.org/10.1002/bem.2250030202.

[36] Mohyud-Din ST, Ali A, Bin-Mohsin B. On biological population model of fractional order. Int J Biomath 2016;09:1650070. https://doi.org/10.1142/S1793524516500704.

[37] Syed M. Approximate analysis of population dynamics with density-dependent migrations and the Allee effects. Int J Num Meth Heat Fluid Flow 2012;22:243–50. https://doi.org/10.1108/09615531211199854.

[38] Ul Hassan QM, Mohyud-Din ST. Investigating biological population model using exp-function method. Int J Biomath 2015;09:1650026. https://doi.org/10.1142/S1793524516500261.

[39] Variational iteration method for nonlinear age-structured population models using auxiliary parameter . Zeitschrift Für Naturforsch A 2010;65:1137. https://doi.org/10.1515/zna-2010-1219.

[40] Iqbal MA, Mohyud-Din ST, Bin-Mohsin B. A study of nonlinear biochemical reaction model. Int J Biomath 2016;09:1650071. https://doi.org/10.1142/S1793524516500716.

[41] Khan U, Ahmed N, Mohyud-Din ST, Bin-Mohsin B. A bio-convection model for MHD flow and heat transfer over a porous wedge containing nanoparticles and gyrotactic microorganisms. J Biol Syst 2016;24:409–29. https://doi.org/10.1142/S0218339016500212.

[42] Pfeifer GP, Besaratinia A. UV wavelength-dependent DNA damage and human non-melanoma and melanoma skin cancer. Photochem Photobiol Sci 2012;11:90–7. https://doi.org/10.1039/C1PP05144J.

[43] Holick MF. Biological Effects of sunlight, ultraviolet radiation, visible light, infrared radiation and vitamin D for health. Anticancer Res 2016;36:1345–56.

[44] Kligman AM. Early destructive effect of sunlight on human skin. JAMA 1969;210:2377–80. https://doi.org/10.1001/jama.1969.03160390039008.

[45] Setlow RB. The wavelengths in sunlight effective in producing skin cancer: a theoretical analysis. Proc Natl Acad Sci 1974;71:3363 LP–6 LP. https://doi.org/10.1073/pnas.71.9.3363.

[46] Mumtaz S, Lim JS, Ghimire B, Lee SW, Choi JJ, Choi EH. Enhancing the power of high power microwaves by using zone plate and investigations for the position of virtual cathode inside the drift tube. Phys Plasmas 2018;25:103113. https://doi.org/10.1063/1.5043595.

[47] Choi E-H, Choi M-C, Jung Y, Choug M-W, Ko J-J, Seo Y, et al. High-power microwave generation from an axially extracted virtual cathode oscillator. IEEE Trans Plasma Sci 2000;28:2128–34. https://doi.org/10.1109/27.902240.

[48] Mumtaz S, Lamichhane P, Sup Lim J, Ho Yoon S, Hyun Jang J, DoyoungKim, et al. Enhancement in the power of microwaves by the interference with a cone-shaped reflector in an axial vircator. Res Phys 2019:102611. https://doi.org/10.1016/j.rinp.2019.102611.

[49] Adhikari M, Adhikari B, Kaushik N, Lee S-J, Kaushik KN, Choi HE. Melanoma growth analysis in blood serum and tissue using xenograft model with response to cold atmospheric plasma activated medium. Appl Sci 2019;9. https://doi.org/10.3390/app9204227.

[50] Li GC, Mivechi NF, Weitzel G. Heat shock proteins, thermotolerance, and their relevance to clinical hyperthermia. Int J Hyperth Off J Eur Soc Hyperther Oncol North Am Hyperth Gr 1995;11:459–88.

[51] Kampinga HH, Brunsting JF, Stege GJJ, Burgman PWJJ, Konings AWT. Thermal protein denaturation and protein aggregation in cells made thermotolerant by various chemicals: role of heat shock proteins. Exp Cell Res 1995;219:536–46. https://doi.org/10.1006/excr.1995.1262.

[52] Yonezawa M, Otsuka T, Matsui N, Tsuji H, Kato KH, Moriyama A, et al. Hyperthermia induces apoptosis in malignant fibrous histiocytoma cells in vitro. Int J Cancer 1996;66:347–51. https://doi.org/10.1002/(SICI)1097-0215(19960503)66:3<347::AID-IJC14>3.0.CO;2-8.

[53] Antico Arciuch VG, Elguero ME, Poderoso JJ, Carreras MC. Mitochondrial regulation of cell cycle and proliferation. Antioxid Redox Sign 2012;16:1150–80. https://doi.org/10.1089/ars.2011.4085.

[54] Zhou Y, Tozzi F, Chen J, Fan F, Xia L, Wang J, et al. Intracellular ATP levels are a pivotal determinant of chemoresistance in colon cancer cells. Cancer Res 2012;72:304 LP–14 LP. https://doi.org/10.1158/0008-5472.CAN-11-1674.

[55] Song S, Jacobson KN, McDermott KM, Reddy SP, Cress AE, Tang H, et al. ATP promotes cell survival via regulation of cytosolic [Ca2+] and Bcl-2/Bax ratio in lung cancer cells. Am J Physiol Physiol 2015;310:C99–C114. https://doi.org/10.1152/ajpcell.00092.2015.

[56] Lomakina GY, Modestova YA, Ugarova NN. Bioluminescence assay for cell viability. Biochemistry (Moscow) 2015;80:701–13. https://doi.org/10.1134/S0006297915060061.

[57] Posimo JM, Unnithan AS, Gleixner AM, Choi HJ, Jiang Y, Pulugulla SH, et al. Viability assays for cells in culture. JoVE 2014:e50645. https://doi.org/10.3791/50645.

[58] Holley AK, Dhar SK, St Clair DK. Curbing cancer's sweet tooth: is there a role for MnSOD in regulation of the Warburg effect?. Mitochondrion 2013;13:170–88. https://doi.org/10.1016/j.mito.2012.07.104.

[59] Xu Y, Miriyala S, Fang F, Bakthavatchalu V, Noel T, Schell DM, et al. Manganese superoxide dismutase deficiency triggers mitochondrial uncoupling and the Warburg effect. Oncogene 2014;34:4229.

[60] Lim J-H, Luo C, Vazquez F, Puigserver P. Targeting mitochondrial oxidative metabolism in melanoma causes metabolic compensation through glucose and glutamine utilization. Cancer Res 2014;74:3535 LP–45 LP. https://doi.org/10.1158/0008-5472.CAN-13-2893-T.